Journal of Human Genetics (2015) 60, 709–716

www.nature.com/jhg

ORIGINAL ARTICLE

Overexpression of microRNA-133a inhibits ischemia-reperfusion-induced cardiomyocyte apoptosis by targeting DAPK2

Sheng Li[1], Fang-Yi Xiao[1], Pei-Ren Shan[1], Lan Su[1], De-Liang Chen[2], Jin-Ye Ding[2] and Zhi-Quan Wang[2]

To examine microRNA-133a (miR-133a) endogenous expression in cardiomyocytes after ischemia-reperfusion (I/R) injury and study the effects of miR-133a overexpression on I/R injury-induced cardiomyocyte apoptosis. Dual-Luciferase Reporter Assay detected dynamic expression of miR-133a. In an *in vitro* hypoxia-reoxygenation (HR) injury model and an *in vivo* rat model of I/R injury, rat cardiomyocytes were transfected with miR-133a mimic to test the effects of miR-133a overexpression on apoptosis. MiR-133a and Death Associated Protein Kinase 2 (DAPK2) mRNA expression was measured using real-time-PCR, and DAPK2 protein expression was detected by western blotting. Annexin V-fluorescein isothiocyanate/propidium iodide (PI) double-staining measured the apoptosis rate in H9C2 cells and transferase dUTP nick end labeling assay quantified the cardiomyocyte apoptosis rate in tissues obtained from *in vivo* the rat model. DAPK2 is a target of miR-133a. Both *in vitro* and *in vivo* results confirmed that after expression of miR-133a mimics, miR-133a levels increased, which was accompanied by decrease in DAPK2 mRNA and protein expression. In H9C2 cells, HR injury caused a sharp decrease in miR-133a expression and a significant upregualtion of DAPK2 mRNA and protein levels. However, exogenous miR-133a expression led to a significant reduction in DAPK2 mRNA and protein levels despite HR injury. Similar results were obtained from *in vivo* I/R injury model. After HR injury or I/R injury the apoptosis rate of myocardial cells was highly elevated and decreased significantly only after transfection of miR-133a into cardiomyocytes. MiR-133a overexpression may inhibit I/R injury-mediated cardiomyocyte apoptosis by targeting DAPK2, leading to reduced DAPK2 protein, thus miR-133a may potentially have a high therapeutic value in I/R injury.
Journal of Human Genetics (2015) **60,** 709–716; doi:10.1038/jhg.2015.96; published online 3 September 2015

INTRODUCTION

Ischemic heart diseases (IHD) remain one of the leading causes of death and long-term morbidity worldwide. World Health Organization projections of global mortality and disease burden for the 2002–2030 period estimates that the economic and health burden associated with IHD will steadily increase in most populations globally.[1] The current therapeutic strategy for IHD is reperfusion of the occluded artery. Paradoxically, reperfusion of ischemic tissues induces severe tissue injury and is termed as myocardial ischemia-reperfusion (I/R) injury.[2–4] I/R injury can cause cardiomyocyte death and has a major impact on ventricular remodeling. I/R injury is associated with adverse cardiovascular outcomes in IHD patients, including progressive deterioration of cardiac function, heart failure and even death.[5,6] In order to find effective therapeutic approaches to reduce adverse outcomes, previous studies investigated the underlying molecular mechanism(s) in myocardial I/R injury-mediated cardiomyocyte death or apoptosis.[7–9] An exciting area of research with a high potential to effectively address treatment of I/R injury involves microRNAs (miRs), as recent evidence shows that cardiac injury and dysfunction caused by I/R injury is regulated by specific miRs. Thus, miRs are being explored as potential therapeutic agents for myocardial I/R injury in IHD patients.[10–12]

MiRs have critical roles in the origin and development of cardiovascular diseases.[12–14] In addition, increasing evidence indicates that miRs control a significant portion of the cellular pathways involved in I/R injury in different organs in humans, for example, in the brain, kidney and small intestine, and the current animal models replicate these injuries and are useful tools to understand the human condition.[15] With specific relevance to miRs, increased miR-133 expression protects against cardiac hypertrophy, which involves remodeling of the heart in response to diverse pathological stimuli, and thus miR-133 may participate in pathways involved in acute stress responses by cardiac tissues.[16] Specifically, as a muscle specific-miRNA of the miR-133 family, miR-133a has important roles in myogenesis, cardiac development and hypertrophy, and the expression level of miR-133a is significantly reduced in infarcted myocardium.[17–19] The significance of this reduction and its exact relevance to cardiac injury remains unknown. However, the miRBase database provides useful information about putative mRNA targets of miR-133a. Based on the functional pathways of these targets, it is proposed that miR-133a may inhibit

[1]Department of Cardiology, the First Affiliated Hospital of Wenzhou Medical University, Wenzhou, China and [2]Department of Cardiology, the Fifth Hospital of Shanxi Medical University, Taiyuan, China
Correspondence: Dr L Su, Department of Cardiology, the First Affiliated Hospital of Wenzhou Medical University, Ouhai District, Wenzhou 325000, China.
E-mail: sulansll_sl0408@126.com
Received 9 December 2014; revised 25 May 2015; accepted 30 June 2015; published online 3 September 2015

cardiomyocyte proliferation, connective tissue growth factor expression and cardiac apoptosis.[16,17,20–22] Further, a previous study showed that miR-133a represses cardiac pacemaker channel genes *HCN2* and *HERG K* (+), known as cardiac potassium channels, thereby protecting cardiac function.[23–26] In this study, we developed hypoxia-reoxygenation (HR) injury model in H9C2 cells and rat I/R injury model to investigate the role of miR-133a in cardiomyocyte apoptosis after HR injury or I/R injury, respectively, to test potential approaches to treat I/R injury and IHD.

MATERIALS AND METHODS

Luciferase reporter assay

To predict targets with significant change, three algorithms (TargetScan, PicTar and microRNA.org) were used for rno-miR-133a. The 3′UTR of Death Associated Protein Kinase 2 (DAPK2) was predicted to interact with rno-miR-133a and therefore this region was amplified by real-time (RT)-PCR and cloned downstream of luciferase gene in GV126 vector (Promega, Madison, WI, USA). Site-directed mutagenesis of rno-miR-133a target-site was carried out to abolish miR-133a binding in 3′ UTR of DAPK2 and pRL-TK (Promega) was used as internal control for dual luciferase assays. HEK293 cells were transfected with miR-133a mimics, along with mutant DAPK2 reporter vector (containing mutant DAPK2 3′ UTR), the negative control (NC) and pRL-TK control vector, as needed within the experimental setup. Luciferase activities were assayed with Dual-Luciferase Reporter Assay kit (Promega). All procedures were performed on the basis of the manufacturer's instructions.

Cell culture and cell transfection

Rat cardiomyocyte cell line H9C2 was bought from American Type Culture Collection (Manassas, VA, USA). Cells were cultured in Dulbecco's modified Eagle's medium with 10% fetal bovine serum in 100-mm culture dishes and were subcultured at 50–60% confluence. H9C2 cells were detached and plated at 5×10^4 cells per well into six well plates. Cells were distributed into six groups: (1) control group: cells cultured under normal oxygen conditions; (2) control+NC group: cells transfected with NC and cultured under normal oxygen conditions; (3) control+miR-133a group: cells transfected with miR-133a and cultured under normal oxygen conditions; (4) HR group: cells were cultured in 2 h of reoxygenation after hypoxia for 10 h; (5) HR+NC group: cells transfected with NC and cultured in 2 h of reoxygenation after hypoxia for 10 h; and (6) HR+miR-133a group: cells transfected with miR-133a mimics and cultured in 2 h of reoxygenation after hypoxia for 10 h. The sense primer for miR-133a mimic was 5′-UUUGGUCCCCUUCAACCAGCUG-3′, and the sense primer for mimics NC was 5′-UCGCUUGGUGCA GGUCGGGAA-3′. Cell transfections were performed using Lipofectamin 2000 (Invitrogen, Carlsbad, California, USA), by following the manufacturer's instructions. The experiment was conducted in triplicates and each experiment was also repeated three times.

HR injury model of cells

H9C2 cells were maintained in Dulbecco's modified Eagle's medium without antibiotics and serum for 12 h and then cultured at 37 °C, 1% O_2, 94% N_2 and 5% CO_2 for 4 h. The medium was changed to Dulbecco's modified Eagle's medium supplemented with 10% fetal bovine serum and the cells were maintained in the Dulbecco's modified Eagle's medium/10% fetal bovine serum at 37 °C, 5% CO_2 for 3 h. Cells were collected for subsequent analysis.

Detection of the miR-133a and DAPK2 mRNA expression by quantitative RT-PCR

Total RNA was extracted from cells using TRIzol Reagent (Invitrogen) following manufacturer's instructions. The quality and concentration of the purified RNA was verified by ultraviolet spectrophotometery (optical density 260/280) and the RNA integrity was verified by agarose gel electrophoresis. Quantitative stem-loop RT-PCR was employed to detect miR-133a and DAPK2 mRNA expression levels. U6 small nuclear RNA was used as an endogenous reference for miR-133a expression and GADPH was used as an endogenous reference for DAPK2. All primers were synthetized at Invitrogen Biotechnology Co., Ltd (Shanghai, China), as listed in Table 1. The Reverse transcription reaction mix contained 1 μg of total RNA, 50 nmol l^{-1} stem-loop primer, 2U of RNAse inhibitor, 5U M-murine leukemia virus (MLV) reverse transcriptase and 0.5 μmol l^{-1} deoxynucleotide triphosphates. The RT reactions were conducted under the following conditions: 16 °C for 30 min, 42 °C for 30 min and 75 °C for 15 min. The quantitative real-time polymerase (qRT)-PCR analyses were carried out in 15 μl and contained 1 μl RT products, 1 × SYBR Green I Master mix (Applied Biosystems, Foster City, CA, USA), 0.5 μmol l^{-1} forward primers, 0.5 μmol l^{-1} reverse primers. The qRT-PCR reaction conditions were 95 °C for 10 min and 40 cycles of 95 °C for 15 s and 60 °C for 1 min. All PCR reactions were performed using Applied Biosystems 7500 RT-PCR system (Applied Biosystems). All RT-PCRs were performed in triplicates. Melting curve analysis and further gel analysis by 3.5% NuSieve agarose electrophoresis (Cambrex, Walkersville, MD, USA) were performed to verify the specificity of the PCR products. All PCR products were analyzed using Opticon Monitor 3 analysis software (Bio-Rad Laboratories, Hercules, CA, USA). The cycle number at threshold (Ct value) was used to calculate the relative amount of mRNA molecules. The results were presented as fold change, calculated using the $2-\Delta\Delta$Ct method.[27]

Detection of the DAPK2 protein expression by western blotting

Western blot analysis was used to detect DAPK2 protein level. Cells or tissues were lysed in protein extraction buffer and the protein concentration was estimated by bicinchoninic acid assay. Total protein (50 μg) was separated by 10% sodium dodecyl sulfate-polyacrylamide gel electrophoresis using constant voltage, followed by protein transfer to polyvinylidene fluoride membrane (Millipore, Belfor, MA, USA). Membranes were blocked with 5% non-fat dry milk at room temperature for 20 min and subsequently, incubated with primary antibodies (DAPK2: ab51601, 1:1000; β-actin: ab6276, 1:5000) in the above solution on an orbital shaker at 4 °C overnight. Following primary antibody incubations, membranes were washed three times and incubated with horseradish peroxidase-linked secondary antibodies (goat anti–rabbit Immunoglobulin G : ab6721, 1:2000; Abcam, Cambridge, UK) for 1 h at room temperature, and visualized using enhanced chemiluminescence (ECL) Plus chemiluminescence (Amersham Biosciences, Piscataway, NJ, USA). Gel Documentation System (Synegene, Frederick, MD, USA) was used to identify the bands in the gels with GeneTools (Synegene).

Assessment of apoptosis by Annexin V-fluorescein isothiocanate (FITC)/PI double-staining

H9C2 cells were detached with trypsin and washed two times with phosphate-buffered saline. Approximately, $1–5\times10^5$ cells were collected in an Eppendorf

Table 1 The primer sequences of RT-PCR amplification of miR-133a and DAPK2

Genes	*Primer sequence*
miR-133a	
Forward	5′-ATGGTTCGTGCGTTTGGTCCCCTTCA-3′
Reverse	5′-GCAGGGTCCGAGGTATTC-3′
U6	
Forward	5′-GCTTCGGCAGCACATATACTAAAAT-3′
Reverse	5′-CGCTTCACGAATTTGCGTGTCAT-3′
DAPK2	
Forward	5′-TCCTGGATGGGGTGAACTAC-3′
Reverse	5′-CAGCTTGATGTGTGGAATGG-3′
GAPDH	
Forward	5′-AGCCACATCGCTCAGACAC-3′
Reverse	5′-GCCCAATACGACCAAATCC-3′

Abbreviations: DAPK2, death associated protein kinase 2; miR-133a, microRNA-133a; U6 and GAPDH, endogenous references.

tube, washed twice with phosphate-buffered saline with centrifugation steps at 2000 rpm for 5 min each. Next, cells were resuspended in 500 μl of binding buffer with 5 μl of Annexin V-FITC. The cells were incubated with 5 μl PI in dark for 5–15 min at room temperature and analyzed within 1 h. Annexin V-FITC and PI emissions were detected in FL1 and FL3 channels, respectively. The apoptotic cells were quantified by flow cytometry (Becton Dickinson, Mountainview, CA, USA). Cells were excited at 488 nm and FITC emission at 515 nm and PI were passed through 560 nm band-pass filters. Both horizontal and vertical coordinates represented the fluorescence intensity of PI and Annexin V-FITC. Viable cells exhibit FITC − /PI − (low left hand quadrant in the plot). Early apoptotic cells exhibit FITC+/PI − (lower right quadrant in the plot), and the late apoptotic cells and necrotic cells exhibit FITC+/PI+ (upper right quadrant in the plot).

Experiment grouping

A total of 60 Wistar rats (female, 12–16 weeks, weighing from 320–350 g) were obtained from the Experimental Animal Center of Shandong University. The animals were housed at constant temperature 2 °C and humidity 60%, under a 12 h light/dark cycle. Sterilized food and water were available *ad libitum*. All animal experimental procedures were performed after obtaining prior approvals from the Institutional Animal Care and Use Committee of the First Affiliated Hospital of Wenzhou Medical University. Reasonable efforts were made to minimize the suffering of animals during all experiments. The rats were randomly divided into three groups: (1) sham-operation group ($n=10$): a silk suture was threaded under the left coronary artery anterior descending without coronary artery ligation and rats were laid for 150 min; (2) NC group ($n=10$): empty virus was directly injected into the myocardium; (3) miR-133a group ($n=10$): rats were injected directly with virus expressing miR-133a mimic; (4) I/R group ($n=10$): the rats were operated upon with ischemia for 60 min followed by 120 min reperfusion; (5) I/R+control group ($n=10$): rats were injected with empty virus and 7 days later underwent the same procedure described in the I/R group; (6) I/R+miR-133a group ($n=10$): rats were injected directly with virus that expressed miR-133a mimic and 7 days later underwent the same procedure described for I/R group. Rats were anesthetized by pentobarbital sodium (50 mg kg^{-1}, ip), intubated and ventilated with a small-animal ventilator with room air at a rate of 60 cycles per minutes. Before surgical operation, the hair on the chests of the rats was shaved and the naked skin was sterilized with iodophors. The tissue and muscle were separated at the left parasternal fourth intercostal space of the rats and the pericardium was opened. Empty virus and virus expressing miR-133a mimic was respectively injected at four points of the anterior myocardial wall in the left ventricle of rats using sterile micro-syringe.

Animal model of I/R injury

After anterior thoracotomy was performed, the left coronary artery anterior descending coronary artery was ligated ~ 1–2 mm distal from its origin with a 4/0 suture. The sternum, muscle layers and skin were then quickly closed. The electrocardiogram was synchronously recorded until the end of this operation. ST segment elevations or the reduction of ST segment suggested successful ligation of coronary artery and the darkened myocardium distal to the ligation line indicated myocardial ischemia. After ligation of left coronary artery anterior descending for 30 min, the coronary artery was reperfusion for 120 min.

Animal sacrifice and specimen collection

After mice were killed, the hearts were excised immediately and washed in pre-cooled physiological saline. Myocardial tissue specimens were collected from the left ventricular anterior wall at 2 mm of the left coronary artery anterior descending ligation. The specimens for RT-PCR assay and western blotting were stored at − 80 °C and the specimens for Terminal deoxynucleotidyl transferase dUTP nick end labeling (TUNEL) assay were fixed in 4% paraformldehyde (Sigma, Shanghai, China), followed by routine dehydration, xylene transparency and embedded in paraffin (Sigma).

Detection of apoptosis by the TUNEL assay

TUNEL assay was performed on paraffin-embedded tissue sections following manufacturer's instructions. In brief, the sections of myocardial tissues were placed on polylysine glass slides. The tissues were de-waxed with xylene and washed with phosphate-buffered saline thrice. Samples was incubated with 50 μl TUNEL reaction mixture at 37 °C for 60 min and the slides rinsed three times with phosphate-buffered saline, mounted with anti-fluorescence quenching liquid seal pieces and observed under a fluorescence microscope. The TUNEL-positive cardiac myocytes (brown nuclei) were photographed and counted in five randomly selected microscopic fields per tissue section and the average value was calculated. The apoptosis index was determined within the different groups (number of positive apoptotic myocytes/total number of myocytes counted × 100%).

Statistical analysis

All data were analyzed using SPSS 19.0 software (SPSS, Inc., Chicago, IL, USA). Data were presented as mean ± s.d. and were tested for normality using a modified Shapiro–Wilks test. Comparisons between two groups were made using *t*-test and comparison among groups were made by One-Way ANOVA. Least significant difference-*t*-test was employed to make multiple comparisons between the means of groups. A two-side *P*-value < 0.05 was used to determine the significance.

RESULTS

DAPK2 is a target gene of miR-133a

The TargetScan algorithms (http://www.targetscan.org/) showed that 3′-UTR of *DAPK2* contained a miR-133a-binding site (Figure 1a). To confirm whether miR-133a directly regulated DAPK2 by targeting the 3′-UTR of *DAPK2*, we constructed wild-type and mutant reporter genes of *GV126-DAPK2* 3′-UTR. After HEK293 cells were co-transduced with miR-133a mimics and the reporters, Dual-Luciferase Reporter Assay (Promega) showed that HEK293 cells transfected with miR-133a mimic exhibited reduced luciferase activity by nearly 50% when wild-type *DAPK2* reporter was used, compared with the NC group. As expected, the luciferase activity of mutant *DAPK2* reporter showed no significant change when co-expresed with

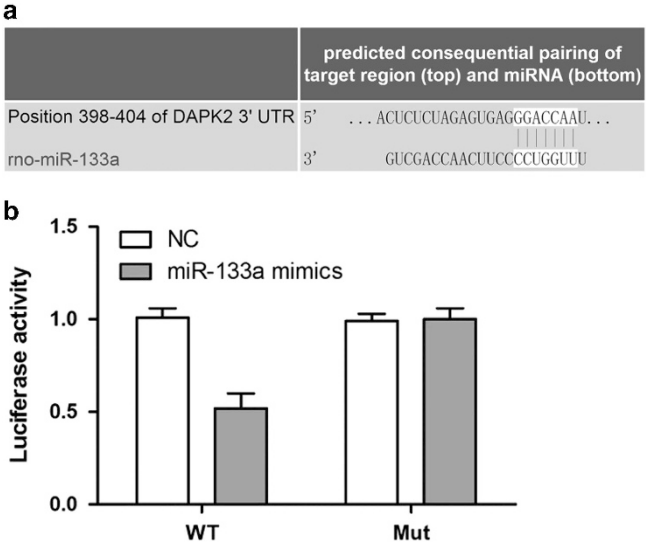

Figure 1 MiR-133a regulates transcriptional activity of *DAPK2* by targeting the 3′-UTR of *DAPK2*. (**a**) TargetScan algorithms showed that the 3′-UTR segment of *DAPK2* gene contains miR-133a-binding site. (**b**) Dual-Luciferase Reporter Assay (Promega) showed that *DAPK2* is the target of miR-133a. A full color version of this figure is available at the *Journal of Human Genetics* journal online.

miR-133a mimics (Figure 1b). These results demonstrated that *DAPK2* is a target of miR-133a.

Transfection efficiency of miR-133a *in vivo* and *in vitro*

The RT-PCR results, representing the transfection efficiency of miR-133a in the *in vivo* and *in vitro* experiments, are illustrated in Figure 2. After transfection with miR-133a mimics for 48 h, miR-133a levels was markedly increased in H9C2 cells, compared with the control group ($P<0.05$), whereas no difference between the control group and control+NC group was observed ($P>0.05$). Similarly, the *in vivo* results revealed that miR-133a expression level in myocardial tissues transfected with miR-133a mimics for 7 days were higher than the sham group ($P<0.05$). As anticipated, the miR-133a level was not significantly different between sham group and NC group ($P>0.05$).

MiR-133a suppressed the expression of DAPK2

The mRNA and protein levels of DAPK2 in H9C2 cells and in rat myocardial tissues in the different groups are shown in Figures 3 and 4, respectively. Compared with the control group, DAPK2 mRNA and protein levels were reduced in H9C2 cells after transfection with miR-133a mimics for 48 h ($P<0.05$). However, control group and control+NC group showed no such changes ($P>0.05$). DAPK2 mRNA and protein levels in the myocardial tissues were detected by RT-PCR and western blotting, respectively, after rats were injected with virus-expressing miR-133a mimic for 7 days. DAPK2 expression decreased significantly in the miR-133a group compared with the sham group ($P<0.05$), whereas no significant difference was found between sham group and NC group ($P>0.05$).

Expression of miR-133a *in vivo* and *in vitro*

In H9C2 cells, miR-133a expression levels in HR group, HR+NC group and HR+miR-133a group were significantly lower compared with the control group (all $P<0.05$), while the miR-133a level in HR +miR-133a group was elevated compared with the HR group and the HR+NC group (both $P<0.05$). There was no significant difference in miR-133a expression level between HR group and HR+NC group ($P>0.05$) (Figure 5). *In vivo* experiment results showed that miR-133a level was elevated in sham group compared with I/R group, I/R +control group and I/R+miR-133a group (all $P<0.05$). MiR-133a level was significantly elevated in I/R+miR-133a group compared with I/R group and I/R+control group (both $P<0.05$). However, miR-133a levels in I/R group and I/R+control group showed no significant differences ($P>0.05$) (Figure 5).

Expression of DAPK2 *in vivo* and *in vitro*

In H9C2 cells, DAPK2 mRNA and protein levels in HR group, HR+NC group and HR+miR-133a group were significantly increased, compared with the control group (all $P<0.05$), whereas the mRNA and protein levels of DAPK2 in the HR+miR-133a group were

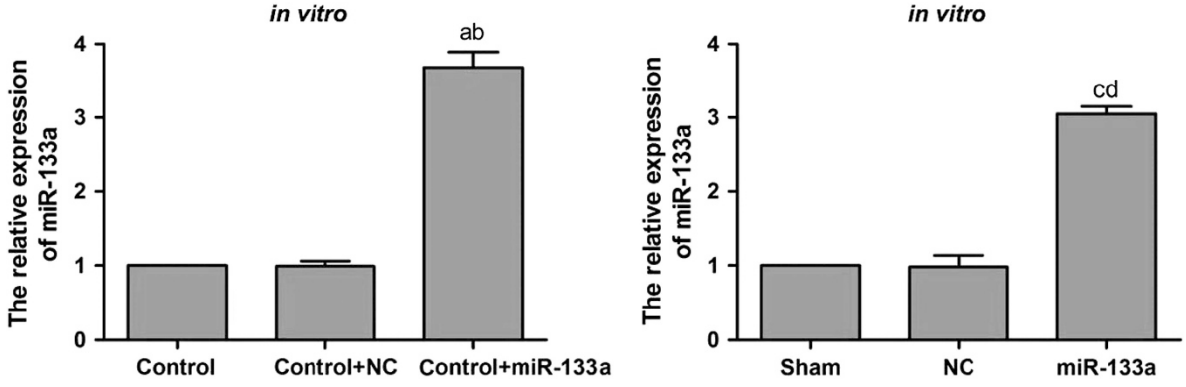

Figure 2 The transfection efficiency of miR-133a in H9C2 cells (*in vitro*) and in myocardial tissue of rats (*in vivo*) quantified by RT-PCR. NC, negative control; RT-PCR, real-time-PCR. Note: (a) compared with control group, $P<0.05$; (b) compared with control+NC group, $P<0.05$; (c) compared with sham group, $P<0.05$; and (d) compared with NC group, $P<0.05$. A full color version of this figure is available at the *Journal of Human Genetics* journal online.

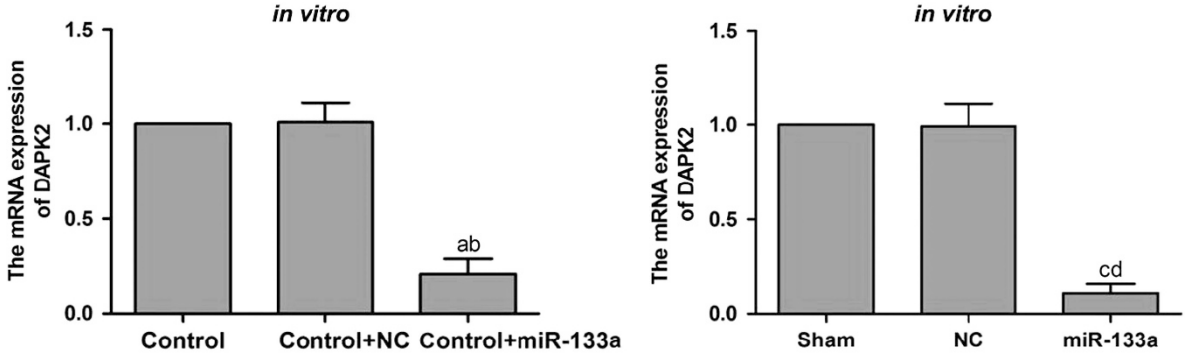

Figure 3 The expression of DAPK2 in H9C2 cells (*in vitro*) and in myocardial tissue of rats (*in vivo*). The RT-PCR results show that miR-133a suppressed the expression of DAPK2. NC, negative control; RT-PCR, real-time-PCR. Note: (a) compared with control group, $P<0.05$; (b) compared with control+NC group, $P<0.05$; (c) compared with sham group, $P<0.05$; and (d) compared with NC group, $P<0.05$. A full color version of this figure is available at the *Journal of Human Genetics* journal online.

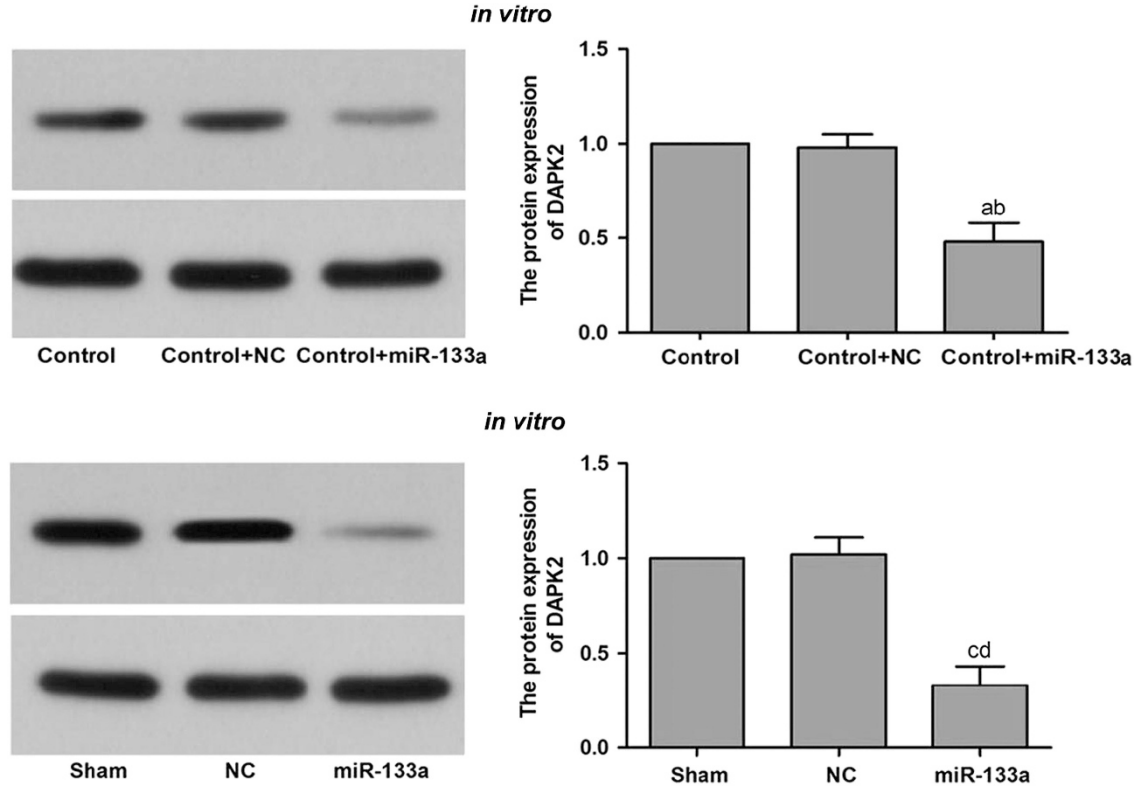

Figure 4 The expression of DAPK2 in H9C2 cells (*in vitro*) and in myocardial tissue of rats (*in vivo*). The western blotting results suggested that the miR-133a suppressed the expression of DAPK2. NC, negative control. Note: (a) compared with control group, $P<0.05$; (b) compared with control+NC group, $P<0.05$; (c) compared with sham group, $P<0.05$; and (d) compared with NC group, $P<0.05$. A full color version of this figure is available at the *Journal of Human Genetics* journal online.

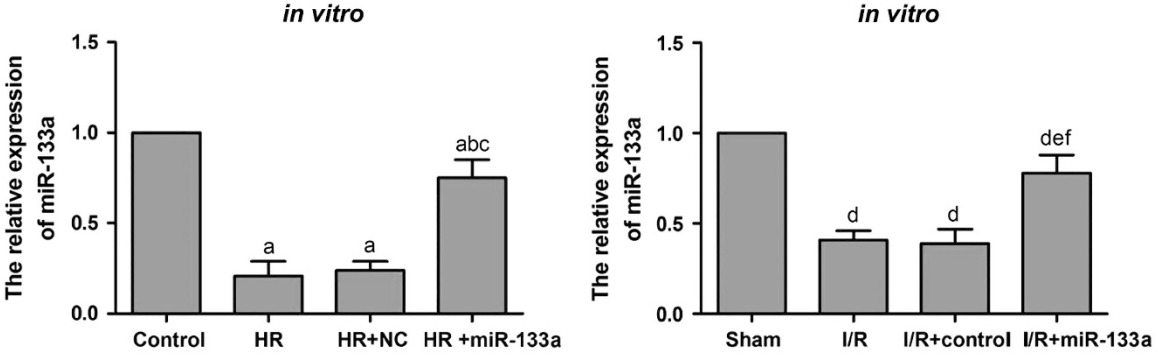

Figure 5 The expression of miR-133a in H9C2 cells after HR treatment (*in vitro*) and in myocardial tissue of I/R rats (*in vivo*). HR, hypoxia-reoxygenation; I/R, ischemia-reperfusion; NC, negative control. Note: (a) compared with control group, $P<0.05$; (b) compared with HR group, $P<0.05$; (c) compared with HR+NC group, $P<0.05$; (d) compared with sham group, $P<0.05$; (e) compared with I/R group, $P<0.05$; and (f) compared with I/R+control group, $P<0.05$. A full color version of this figure is available at the *Journal of Human Genetics* journal online.

downregulated compared to HR group and HR+NC group (both $P<0.05$). No significant differences in DAPK2 mRNA and protein levels were observed between the HR group and HR+NC group ($P>0.05$) (Figures 6 and 7). In comparison to the sham group, DAPK2 mRNA and protein levels were apparently increased in the I/R group, I/R+control group and I/R+miR-133a group (all $P<0.05$), but DAPK2 mRNA and protein level was lower in I/R +miR-133a group compared with the I/R group and I/R+control group (both $P<0.05$). No significant differences in DAPK2 mRNA and protein levels were observed between the I/R group and I/R +control group ($P>0.05$).

MiR-133a inhibited HR-induced apoptosis

As shown by Annexin V-FITC/PI double-staining (Figure 8), the rate of apoptosis in H9C2 cells in the control group was $7.12\pm0.62\%$, which was markedly lower than the HR group, HR+NC group and HR+miR-133a group. There was no significant difference in the rate of apoptosis of H9C2 cells between HR group and HR+NC group

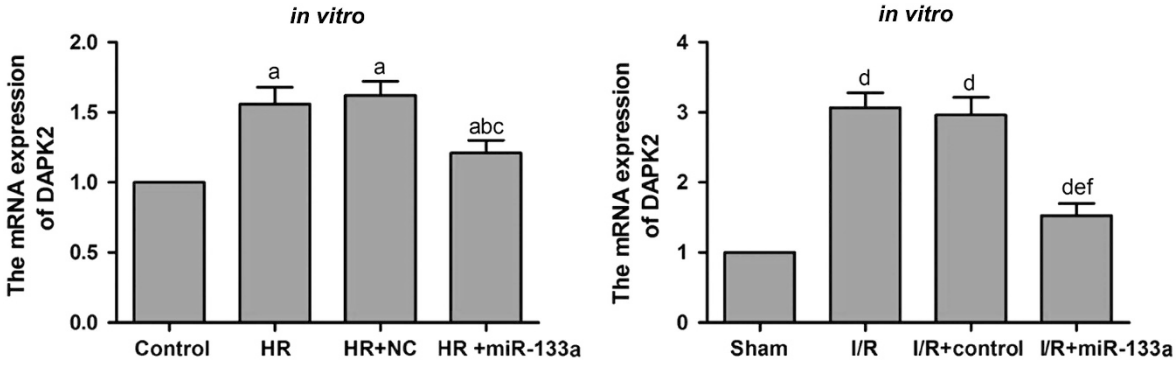

Figure 6 The RT-PCR results of DAPK2 mRNA expression in H9C2 cells after HR treatment (*in vitro*) and in myocardial tissue of I/R rats (*in vivo*). HR: hypoxia-reoxygenation; I/R: ischemia-reperfusion; NC: negative control; RT-PCR, real-time-PCR. Note: (a) compared with control group, $P<0.05$; (b) compared with HR group, $P<0.05$; (c) compared with HR+NC group, $P<0.05$; (d) compared with sham group, $P<0.05$; (e) compared with I/R group, $P<0.05$; and (f) compared with I/R+control group, $P<0.05$. A full color version of this figure is available at the *Journal of Human Genetics* journal online.

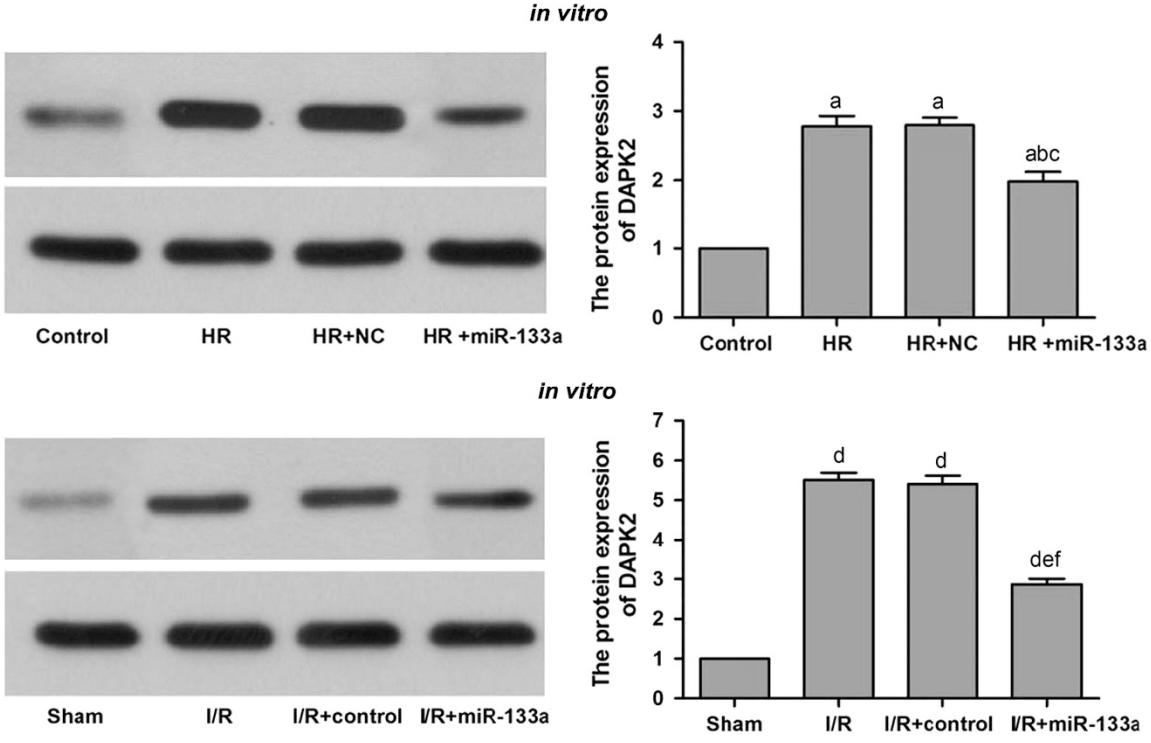

Figure 7 Western blotting results of DAPK2 protein expression in H9C2 cells after HR treatment (*in vitro*) and in myocardial tissue of I/R Wistar rats (*in vivo*). HR: hypoxia-reoxygenation; I/R: ischemia-reperfusion; NC: negative control. Note: (a) compared with control group, $P<0.05$; (b) compared with HR group, $P<0.05$; (c) compared with HR+NC group, $P<0.05$; (d) compared with sham group, $P<0.05$; (e) compared with I/R group, $P<0.05$; and (f) compared with I/R+control group, $P<0.05$. A full color version of this figure is available at the *Journal of Human Genetics* journal online.

(HR group: $22.45\pm2.69\%$ vs HR+NC group: $25.18\pm4.17\%$, $P>0.05$). Further, transfection of miR-133a mimic significantly reduced the rate of apoptosis to 12.45 ± 2.54 compared with the HR +NC group, the rate of apoptosis was significantly decreased in the HR +miR-133a group ($P<0.05$).

Detection of apoptosis by TUNEL staining

As shown by TUNEL staining (Figure 9), the apoptosis rate in sham group was $13.45\pm1.12\%$, whereas the TUNEL-positive cardio myocytes were significantly increased in the I/R group and I/R +control group (I/R group: $35.49\pm1.69\%$; I/R+control group: $36.62\pm1.22\%$). Myocardial tissue of the I/R group exhibited a larger number of TUNEL-positive cells compared with the sham group, whereas the apoptosis rate in the I/R group and I/R+control group exhibited no significant difference ($P>0.05$). However, the apoptosis rate was significantly lower in the I/R+miR-133a group as compared with the I/R+control group ($25.71\pm1.39\%$ vs 36.62 ± 1.22, $P<0.05$).

DISCUSSION

The current study examines the expression of miR-133a in cardiomyocytes after HR injury and I/R injury with the aim of understanding miR-133a function and uncovering the underlying mechanisms in

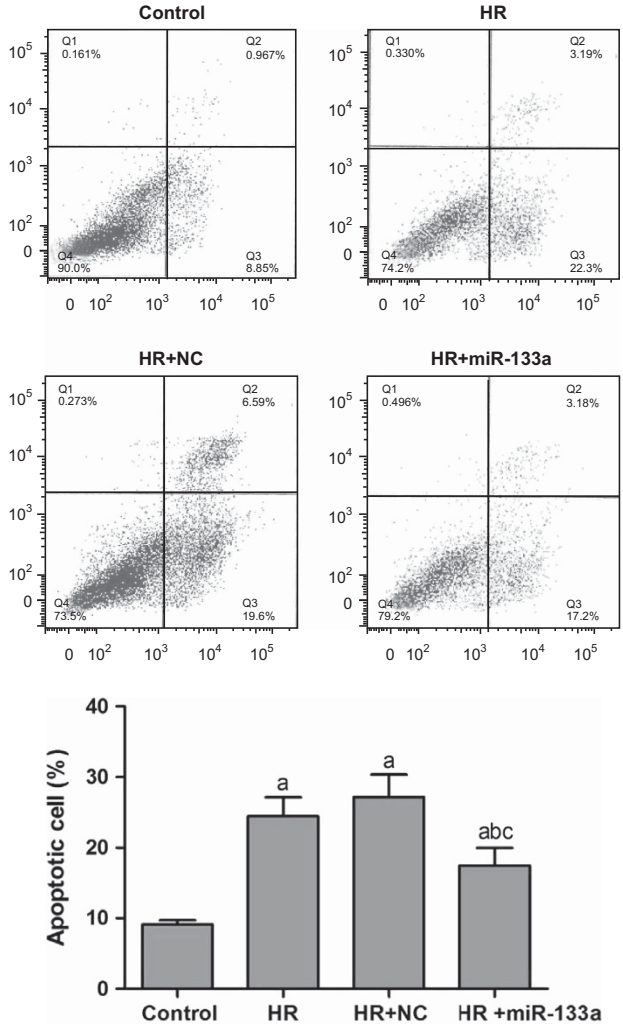

Figure 8 The detection of apoptosis rate of H9C2 cells by Annexin V-FITC/PI double-staining of the control group, HR group, HR+NC group and HR+miR-133a group. FITV, fluorescein isothiocanate; HR: hypoxia-reoxygenation; NC: negative control. Note: (a) compared with control group, $P<0.05$; (b) compared with HR group, $P<0.05$; and (c) compared with HR+NC group, $P<0.05$. A full color version of this figure is available at the *Journal of Human Genetics* journal online.

cardiomyocyte apoptosis induced by HR injury or I/R injury. Our RT-PCR results indicated that miR-133a expression levels decreased in myocardial cells after HR injury or I/R injury. These findings suggest that miR-133a expression level is influenced by myocardial I/R injury and downregulation of miR-133a expression may contribute to myocardial I/R injury. Myocardial I/R injury is implicated in myocardial necrosis and myocardial cell apoptosis, leading to impaired cardiac function.[3] Recently, several miRNAs were identified as crucial players in the progression of heart failure by negatively regulating the expression of target genes that control cardiac remodeling.[12,26] One of the important muscle-specific miRNAs, miR-133a, is specifically expressed in skeletal muscles and cardiomyocytes.[28] MiR-133a is a key regulatory factor in cardiac development, cardiomyocyte differentiation and proliferation.[22] Izarra *et al.*[29] found that miR-1 and miR-133a are upregulated during *in vitro* cardiac differentiation of adult cardiac progenitor cells and the upregulated expression of miR-133a may protect cardiac progenitor cells against apoptosis following myocardial infarction. A clue to the involvement of miR-133a was provided by previous studies that showed miR-133a downregulation during cardiac muscle remodeling and during myocardial I/R injury, cardiac hypertrophy or heart failure.[28,30,31] He *et al.*[32] also demonstrated that miR-133a expression levels decreased within 180 min of reperfusion in a rat I/R injury model, which is consistent with our findings. Our study finds that through exogenous expression of miR-133a, the miR-133a levels can be increased in myocardial cells, both *in vitro* and *in vivo,* to functionally relevant levels sufficient to alter the outcome of I/R injury. It is also worthwhile to note that miR-133a may also promote the differentiation of embryonic stem cells into cardiomyocytes.[33,34] Consistent with our findings, Xu *et al.*[35] have suggested that overexpression of miR-133a decreases cardiomyocyte apoptosis induced by H_2O_2, and thus may improve cardiac function and reduce the risk of further injury to heart. Zhu *et al.*[36] also suggested that upregulation of miR-133 expression levels during an ischemic event might potentially attenuate myocardial I/R injury. Therefore, we propose that miR-133a has a crucial role in preventing cardiomyocyte apoptosis induced by I/R injury and may regulate cardiac development by modulating cardiomyocyte apoptosis.

To identify the underlying mechanisms involved in miR-133a-mediated attenuation of HR or I/R injury, bioinformatic algorithms were used to search for potential miR-133a target genes. The TargetScan results revealed *DAPK2* as a possible target of miR-133a and one miR-133a-binding site was identified within the 3′-UTR of

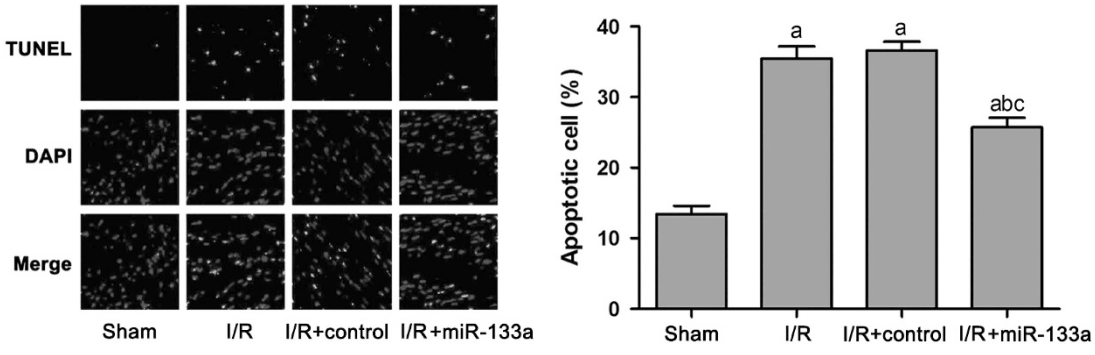

Figure 9 The detection of the apoptosis rate of myocardial cells of rats by TUNEL staining of the sham group, I/R group, I/R+control group and I/R +miR-133a group. I/R: ischemia-reperfusion. Note: (a) compared with sham group, $P<0.05$; (b) compared with I/R group, $P<0.05$; and (c) compared with I/R+control group, $P<0.05$. A full color version of this figure is available at the *Journal of Human Genetics* journal online.

DAPK2 mRNA. DAPK2 belongs to serine/threonine protein kinase family and is a multifunctional protein kinase involved in apoptotic pathways mediated by death receptors.[37] DAPK2 appear to function in downstream signaling pathways which activate NF-κB and p53 and suppression of DAPK2 activity is known to increase the expression levels of DR4 and DR5 TRAIL receptors, sensitizing cells to TRAIL-mediated apoptosis. In cardiomyocytes, DAPK2 may control apoptosis directly or through other receptor mechanisms.[38] In our study, the *in vitro* and *in vivo* results showed we were able to achieve significantly overexpression of miR-133a in cardiomyocytes after transfection of miR-133a mimic, which led to a sharp decrease in DAPK2 mRNA and protein levels. Endogenous miR-133a expression level decreased after HR injury in H9C2 cells and the DAPK2 mRNA and protein levels were elevated. Further, exogenous miR-133 a mimics increased miR-133a level and led to a sharp decrease in DAPK2 mRNA and protein levels. Collectively, these results suggest that DAPK2 level is negatively regulated by miR-133a. The Annexin V-FITC/PI double-staining and TUNEL assay results revealed that HR or I/R injury increased cardiomyocytes apoptosis, but myocardial cells transfected with miR-133a mimics exhibited significantly decreased apoptosis rate. We propose that overexpression miR-133a inhibits cardiomyocyte apoptosis by negatively regulating DAPK2 mRNA and protein levels.

In conclusion, our findings support the view that miR-133a expression in cardiomyocytes is significantly downregulated following I/R injury. Moreover, we identify that miR-133a inhibits HR or I/R injury-mediated cardiomyocyte apoptosis by suppressing DAPK2 mRNA and protein expression. Thus, cardioprotection by miR-133a overexpression may be a potential novel therapeutic approach for treatment of ischemic heart disease.

CONFLICT OF INTEREST

The authors declare no conflict of interest.

ACKNOWLEDGEMENTS

We would like to acknowledge the reviewers for their helpful comments on this paper.

1 Mathers, C. D. & Loncar, D. Projections of global mortality and burden of disease from 2002 to 2030. *PLoS Med.* **3**, e442 (2006).
2 Hausenloy, D. J. & Yellon, D. M. Myocardial ischemia-reperfusion injury: a neglected therapeutic target. *J. Clin. Invest.* **123**, 92–100 (2013).
3 Frank, A., Bonney, M., Bonney, S., Weitzel, L., Koeppen, M. & Eckle, T. Myocardial ischemia reperfusion injury: from basic science to clinical bedside. *Semin. Cardiothorac. Vasc. Anesth.* **16**, 123–132 (2012).
4 Canty, J. M. Jr & Suzuki, G. Myocardial perfusion and contraction in acute ischemia and chronic ischemic heart disease. *J. Mol. Cell. Cardiol.* **52**, 822–831 (2012).
5 Frohlich, G. M., Meier, P., White, S. K., Yellon, D. M. & Hausenloy, D. J. Myocardial reperfusion injury: looking beyond primary PCI. *Eur. Heart J.* **34**, 1714–1722 (2013).
6 Diez, E. R., Altamirano, L. B., Garcia, I. M., Mazzei, L., Prado, N. J., Fornes, M. W. *et al.* Heart remodeling and ischemia-reperfusion arrhythmias linked to myocardial vitamin d receptors deficiency in obstructive nephropathy are reversed by paricalcitol. *J. Cardiovasc. Pharmacol. Ther.* **20**, 211–220 (2014).
7 Hausenloy, D. J. & Yellon, D. M. The therapeutic potential of ischemic conditioning: an update. *Nat. Rev. Cardiol.* **8**, 619–629 (2011).
8 Dongworth, R. K., Mukherjee, U. A., Hall, A. R., Astin, R., Ong, S. B., Yao, Z. *et al.* DJ-1 protects against cell death following acute cardiac ischemia-reperfusion injury. *Cell Death Dis.* **5**, e1082 (2014).
9 Siddall, H. K., Yellon, D. M., Ong, S. B., Mukherjee, U. A., Burke, N., Hall, A. R. *et al.* Loss of PINK1 increases the heart's vulnerability to ischemia-reperfusion injury. *PLoS One* **8**, e62400 (2013).
10 Ren, X. P., Wu, J., Wang, X., Sartor, M. A., Qian, J., Jones, K. *et al.* MicroRNA-320 is involved in the regulation of cardiac ischemia/reperfusion injury by targeting heat-shock protein 20. *Circulation* **119**, 2357–2366 (2009).
11 Cheng, Y., Zhu, P., Yang, J., Liu, X., Dong, S., Wang, X. *et al.* Ischaemic preconditioning-regulated miR-21 protects heart against ischaemia/reperfusion injury via anti-apoptosis through its target PDCD4. *Cardiovasc. Res.* **87**, 431–439 (2010).
12 Di, Y., Lei, Y., Yu, F., Changfeng, F., Song, W. & Xuming, M. MicroRNAs expression and function in cerebral ischemia reperfusion injury. *J. Mol. Neurosci.* **53**, 242–250 (2014).
13 Tutar, L., Tutar, E. & Tutar, Y. MicroRNAs and cancer; an overview. *Curr. Pharm. Biotechnol.* **15**, 430–437 (2014).
14 Olson, E. N. MicroRNAs as therapeutic targets and biomarkers of cardiovascular disease. *Sci. Transl. Med.* **6**, 239ps3 (2014).
15 Ye, Y., Perez-Polo, J. R., Qian, J. & Birnbaum, Y. The role of microRNA in modulating myocardial ischemia-reperfusion injury. *Physiol. Genomics* **43**, 534–542 (2011).
16 Dong, D. L., Chen, C., Huo, R., Wang, N., Li, Z., Tu, Y. J. *et al.* Reciprocal repression between microRNA-133 and calcineurin regulates cardiac hypertrophy: a novel mechanism for progressive cardiac hypertrophy. *Hypertension* **55**, 946–952 (2010).
17 Care, A., Catalucci, D., Felicetti, F., Bonci, D., Addario, A., Gallo, P. *et al.* MicroRNA-133 controls cardiac hypertrophy. *Nat. Med.* **13**, 613–618 (2007).
18 Fichtlscherer, S., De Rosa, S., Fox, H., Schwietz, T., Fischer, A., Liebetrau, C. *et al.* Circulating microRNAs in patients with coronary artery disease. *Circ. Res.* **107**, 677–684 (2010).
19 Kuwabara, Y., Ono, K., Horie, T., Nishi, H., Nagao, K., Kinoshita, M. *et al.* Increased microRNA-1 and microRNA-133a levels in serum of patients with cardiovascular disease indicate myocardial damage. *Circ. Cardiovasc. Genet.* **4**, 446–454 (2011).
20 Duisters, R. F., Tijsen, A. J., Schroen, B., Leenders, J. J., Lentink, V., van der Made, I. *et al.* miR-133 and miR-30 regulate connective tissue growth factor: implications for a role of microRNAs in myocardial matrix remodeling. *Circ. Res.* **104**, 170–178 (2009)
21 Griffiths-Jones, S. miRBase: microRNA sequences and annotation. *Curr. Protoc. Bioinform.* Chapter 12, Unit 12.9.1-10 (2010).
22 Liu, N., Bezprozvannaya, S., Williams, A. H., Qi, X., Richardson, J. A., Bassel-Duby, R. *et al.* microRNA-133a regulates cardiomyocyte proliferation and suppresses smooth muscle gene expression in the heart. *Genes Dev.* **22**, 3242–3254 (2008).
23 Xiao, J., Luo, X., Lin, H., Zhang, Y., Lu, Y., Wang, N. *et al.* MicroRNA miR-133 represses HERG K+ channel expression contributing to QT prolongation in diabetic hearts. *J. Biol. Chem.* **282**, 12363–12367 (2007).
24 Luo, X., Lin, H., Pan, Z., Xiao, J., Zhang, Y., Lu, Y. *et al.* Down-regulation of miR-1/miR-133 contributes to re-expression of pacemaker channel genes HCN2 and HCN4 in hypertrophic heart. *J. Biol. Chem.* **283**, 20045–20052 (2008).
25 Vandenberg, J. I., Perry, M. D., Perrin, M. J., Mann, S. A., Ke, Y. & Hill, A. P. hERG K(+) channels: structure, function, and clinical significance. *Physiol. Rev.* **92**, 1393–1478 (2012).
26 Luo, X., Lin, H., Pan, Z., Xiao, J., Zhang, Y., Lu, Y. *et al.* Down-regulation of miR-1/miR-133 contributes to re-expression of pacemaker channel genes HCN2 and HCN4 in hypertrophic heart. *J. Biol. Chem.* **286**, 28656 (2011).
27 Livak, K. J. & Schmittgen, T. D. Analysis of relative gene expression data using real-time quantitative PCR and the 2(-Delta Delta C(T)) Method. *Methods* **25**, 402–408 (2001).
28 Townley-Tilson, W. H., Callis, T. E. & Wang, D. MicroRNAs 1, 133, and 206: critical factors of skeletal and cardiac muscle development, function, and disease. *Int. J. Biochem. Cell. Biol.* **42**, 1252–1255 (2010).
29 Izarra, A., Moscoso, I., Levent, E., Canon, S., Cerrada, I., Diez-Juan, A. *et al.* miR-133a enhances the protective capacity of cardiac progenitors cells after myocardial infarction. *Stem Cell Rep.* **3**, 1029–1042 (2014).
30 Sayed, D., Hong, C., Chen, I. Y., Lypowy, J. & Abdellatif, M. MicroRNAs play an essential role in the development of cardiac hypertrophy. *Circ. Res.* **100**, 416–424 (2007).
31 Tatsuguchi, M., Seok, H. Y., Callis, T. E., Thomson, J. M., Chen, J. F., Newman, M. *et al.* Expression of microRNAs is dynamically regulated during cardiomyocyte hypertrophy. *J. Mol. Cell. Cardiol.* **42**, 1137–1141 (2007).
32 He, B., Xiao, J., Ren, A. J., Zhang, Y. F., Zhang, H., Chen, M. *et al.* Role of miR-1 and miR-133a in myocardial ischemic postconditioning. *J. Biomed. Sci* **18**, 22 (2011).
33 Ivey, K. N., Muth, A., Arnold, J., King, F. W., Yeh, R. F., Fish, J. E. *et al.* MicroRNA regulation of cell lineages in mouse and human embryonic stem cells. *Cell Stem Cell* **2**, 219–229 (2008).
34 Xu, C., Lu, Y., Pan, Z., Chu, W., Luo, X., Lin, H. *et al.* The muscle-specific microRNAs miR-1 and miR-133 produce opposing effects on apoptosis by targeting HSP60, HSP70 and caspase-9 in cardiomyocytes. *J. Cell Sci.* **124**, 3187 (2011).
35 Xu, C., Lu, Y., Pan, Z., Chu, W., Luo, X., Lin, H. *et al.* The muscle-specific microRNAs miR-1 and miR-133 produce opposing effects on apoptosis by targeting HSP60, HSP70 and caspase-9 in cardiomyocytes. *J. Cell Sci.* **120**, 3045–3052 (2007).
36 Zhu, H. & Fan, G. C. Role of microRNAs in the reperfused myocardium towards post-infarct remodelling. *Cardiovasc. Res.* **94**, 284–292 (2012).
37 Lin, Y., Hupp, T. R. & Stevens, C. Death-associated protein kinase (DAPK) and signal transduction: additional roles beyond cell death. *FEBS J.* **277**, 48–57 (2010).
38 Britschgi, A., Trinh, E., Rizzi, M., Jenal, M., Ress, A., Tobler, A. *et al.* DAPK2 is a novel E2F1/KLF6 target gene involved in their proapoptotic function. *Oncogene* **27**, 5706–5716 (2008).